# Corrosion protection of copper by self assembled monolayers

B V Appa Rao[a]*, K Chaitanya Kumar[a], Md Yakub Iqbal[a] & B Sreedhar[b]

[a]Department of Chemistry, National Institute of Technology, Warangal 506 004, India

[b]Inorganic & Physical Chemistry Division, Indian Institute of Chemical Technology, Hyderabad 500 007, India

Email: boyapativapparao@rediffmail.com

Self assembled monolayer (SAM) of 3-methyl-5-octadecylsulfanyl-[1,2,4]triazole-4-ylamine (MOSTY) was formed on the copper surface and the optimum conditions of formation of SAM were established. Corrosion behaviour of copper with the SAM was investigated in 0.02 M aq. HCl (acidic) and 0.02 M aq. NaCl (neutral) solutions. Weight-loss measurements, potentiodynamic polarization studies and electrochemical impedance studies were carried out in order to investigate the effect of MOSTY SAM on the corrosion protection of copper. Appropriate equivalent circuit models were used for impedance measurements of bare copper and the SAM covered copper in the chosen aggressive environments. These studies revealed the corrosion inhibition efficiency of SAM to an extent of 98% in 0.02 M aq. NaCl and 86% in 0.02 M aq. HCl environments. Potentiodynamic polarization studies revealed that this SAM controls both the anodic and cathodic reactions and thus protects copper from corrosion. The X-ray photoelectron spectroscopy (XPS) was used to characterize the SAM. The XPS revealed the presence of various elements *viz.* carbon, nitrogen and sulphur in the SAM. Shifts in binding energies of nitrogen and sulphur were interpreted. The inhibition of copper dissolution was interpreted due to the chelating effect of Cu (I) ions with the chemisorbed ligand molecules forming a complex of SAM on copper surface.

**Keywords:** Self assembled monolayer, 3-Methyl-5-octadecylsulfanyl-[1,2,4]triazole-4-ylamine, Copper, Corrosion inhibition

Considerable attention has been drawn during the past few decades to inhibit corrosion of copper, as it has wide application in industry. Copper is used in microelectronics, fabrication of heat exchanger tubes and cooling water systems, due to its high thermal and electrical conductivities, low cost and malleability[1-3]. Corrosion inhibition of copper can be achieved through the modification of its surface by forming self assembled ordered ultrathin layers of organic inhibitors. The strong chemical interaction between sulphur atoms and the metallic surfaces leads to robust and easy preparation of chemisorbed organic films[1]. The widely used organic inhibitors are nitrogen and/or sulphur containing heterocyclic compounds[3,4]. The advantages of SAMs include simplicity of preparation, versatility, stability, reproducibility and the possibility of introducing different chemical functionalities with high level of order on a molecular dimension[5-7]. The SAMs of organic molecules are found to produce effective barriers to the penetration of corrosive chemicals to the copper surface and to limit the oxidation of copper metal[8]. Feng *et al.*[9] and Itoh *et al.*[10] studied the corrosion resistance offered by SAM of alkanethiol to copper in different aggressive environments. The maximum efficiency up to 80.3% of the self assembled monolayer of octadecanethiol on copper for inhibition of corrosion in 0.5 M $Na_2SO_4$ solution was reported by Yamamoto *et al.*[11]. Laibinis and Whitesides[12] studied the effective inhibition property of the SAMs of alkanethiols on copper corrosion in air. Quan *et al.*[13, 14] studied the corrosion protection of copper by forming self assembled monolayers of schiff bases. Tremont *et al.*[15] reported the inhibiting properties of 3-mercaptopropyltrimethoxysilane, propyltrimethoxysilane, and 1-propanethiol on copper corrosion in 0.10 M KCl aqueous solution, in the presence of oxygen.

The aim of the present study is to investigate the ability of SAM of 3-methyl-5-octadecylsulfanyl-[1,2,4]triazole-4-ylamine (MOSTY) to inhibit copper corrosion in 0.02 M aq. HCl and 0.02 M aq. NaCl environments. Weight-loss, potentiodynamic polarization and electrochemical impedance studies were carried out in order to calculate the inhibition efficiency (IE)[9,16,17]. The stable and protective monolayer present on the copper surface was analyzed by X-ray photoelectron spectroscopy (XPS).

## Experimental Procedure

Formation of self assembled monolayer of MOSTY on copper was carried out with the following steps.

Synthesis of 3-methyl-5-octadecylsulfanyl-[1,2,4]tri-azole-4-ylamine (MOSTY) was a 2 step process. In the first step 4-amino-5-methyl-4H-[1,2,4]triazole-3-thiol was prepared by using the procedures available in the literature[18-20]. In the second step MOSTY was synthesized by adding octadecyl chain to 4-amino-5-methyl-4H-[1,2,4]triazole-3-thiol. The structure of the compound is shown in Fig. 1.

Appropriate quantity of MOSTY was dissolved in chloroform to get a 10 mM solution. The copper specimens were taken from the 99 wt. % pure copper sheet. These specimens, with the dimensions of 4.0×1.0×0.2 cm, were polished to mirror finish using 2/0, 3/0 and 4/0 grade emery papers and degreased with acetone. The polished copper specimens were etched with 7 N HNO$_3$ for 30 s, washed with triple distilled water and then with chloroform. These specimens were then immersed in 10 mM MOSTY solution in chloroform for two different immersion periods *viz.* 12 h and 24 h. The MOSTY SAM formed after 24 h immersion period was found to have very high impedance and hence chosen for the corrosion studies. The two different corrosive environments used in this study were 0.02 M aq. HCl and 0.02 M aq. NaCl solutions. These environments were prepared by using analytical grade chemicals and triple distilled water.

The inhibition efficiencies of the SAM were determined by weight-loss method. The bare copper specimens in duplicate and the copper specimens with SAM in duplicates were immersed in 0.02 M aq. HCl and 0.02 M aq. NaCl solutions for a period of 3 days. The weights of the specimens, before and after immersion were recorded by using an electronic balance with a readability of 0.01 mg. The corrosion rates and inhibition efficiencies were calculated from the weight-loss data.

The potentiodynamic polarization studies were carried out in a three-electrode cell assembly at room temperature (30°C) using a Zahner IM6e electrochemica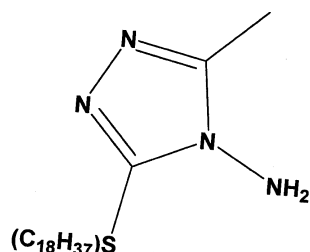l work station. The bare copper specimen or copper specimen with SAM was used as the working electrode. Platinum was used as the counter electrode and the reference electrode was a silver-silver chloride electrode. The studies were made in the potential range of −0.500 to +0.200 V versus Ag/AgCl.

The impedance studies were also carried out by using the same 3 electrode cell assembly and the electrochemical work station as described above. The impedance measurements were carried out at the open-circuit potential ($E_{oc}$) in the frequency range from 60 kHz to 10 mHz. The inhibition efficiencies of SAM were calculated by the potentiodynamic polarization and impedance studies also. The SAM formed on the copper surface was analyzed by using the X-ray photoelectron spectrophotometer, ESCA Kratos model AXIS-155, with Mg Kα radiation. Computer deconvolution was applied to detect the elemental peaks of nitrogen, sulphur and carbon present in the SAM.

## Results and Discussion

### Weight-loss studies

The corrosion rates have been expressed in mg dm$^{-2}$ day$^{-1}$. The inhibition efficiencies (IE) of the SAM covered copper have been calculated by using Eq. (1)[21].

$$IE = (\Delta W - \Delta W_1) \times 100 / \Delta W \qquad \ldots(1)$$

where $\Delta W$ and $\Delta W_1$ are the weight losses of the bare copper and SAM covered copper respectively in the corrosive environments. The obtained inhibitory efficiencies are shown in the Table 1. The inhibition efficiencies as high as 86.7% in 0.02 M aq. HCl and 92.7% in 0.02 M aq. NaCl environments, infer that the MOSTY SAM on the copper surface offers a good corrosion protection. The relative standard deviation in corrosion rate determinations is of the order of 2% (ref. 22).



Fig. 1 — Structure of 3-methyl-5-octadecylsulfanyl-[1,2,4]triazole-4-ylamine

Table 1 — Corrosion rates from weight-loss studies

| S. No | Specimen | Corrosive environment | Weight loss (mg) | Corrosion rate (mdd) | IE (%) |
|-------|----------|----------------------|------------------|---------------------|--------|
| 1 | Bare copper | 0.02 M HCl | 10.8 | 36.0 | -- |
| 2 | SAM covered copper | 0.02 M HCl | 1.4 | 4.8 | 86.7 |
| 3 | Bare copper | 0.02 M NaCl | 5.7 | 19.2 | -- |
| 4 | SAM covered copper | 0.02 M NaCl | 0.4 | 1.4 | 92.7 |

**Potentiodynamic polarization studies**

The potentiodynamic polarization curves of bare copper and SAM covered copper specimen in 0.02 M HCl solution are shown in Fig. 2. The corrosion potential ($E_{corr}$) for bare copper is found to be −42.77 mV versus Ag/AgCl which is shifted towards cathodic side to a value of −165.4 mV versus Ag/AgCl, when the copper is covered with SAM. The corrosion current densities for bare copper and MOSTY SAM covered copper in 0.02 M HCl are 13.1 and 1.64 µA respectively. Thus there is a large decrease in the corrosion current density in the presence of SAM, which reveals that the MOSTY SAM protects copper from corrosion. The anodic and cathodic Tafel slopes for bare copper in 0.02 M HCl are found to be 46.6 and −591.0 mV/decade respectively. When the copper surface is covered with SAM, these slopes are shifted to 88.3 and −115.0 mV/decade respectively. Thus, a shift in both the anodic and cathodic Tafel slopes was observed. This reveals that the MOSTY SAM controls both the anodic and cathodic reactions. But it controls more the cathodic reaction, because the cathodic slope is shifted to a larger extent than the anodic slope. Figure 3 shows the potentiodynamic polarization curves of the bare copper and MOSTY SAM covered copper specimen in 0.02 M NaCl solution. The corrosion potential ($E_{corr}$) for bare copper is found to be -83.5 mV versus Ag/AgCl, which is shifted to the cathodic side to a value of -132.9 mV versus Ag/AgCl when the metal is covered with SAM. The corrosion current densities for bare copper and MOSTY SAM covered copper in 0.02 M NaCl are 11.9 and 0.205 µA respectively. There is a huge decrease in the corrosion current density, which reveals that the MOSTY SAM inhibits the corrosion reaction of copper. The anodic and cathodic Tafel slopes for bare copper specimen are 80.8 and −433 mV/decade respectively. The anodic and cathodic Tafel slopes for the SAM covered copper are found to be 128.0 and −133 mV/decade and there is a large shift in the cathodic slope. This concludes that the MOSTY SAM inhibits the cathodic reaction to a larger extent than the anodic, though it controls both anodic and cathodic reactions.

Based on Lee and Nobe[23-26] model, the anodic dissolution of copper can be represented by a 2 step process as given in Eqs (2) and (3).

1st step: $Cu + Cl^- \rightarrow CuCl + e^-$ ...(2)

2nd step: $CuCl + Cl^- \rightarrow CuCl_2^-$ ...(3)

Here CuCl is an insoluble adsorbed species. The diffusion rate of the soluble $CuCl_2^-$ species explains the dissolution process. The $CuCl_2^-$ species diffuses from the electrode surface into bulk of the solution. This results in an apparent anodic slope of 2.303 $RT/F$[27]. The copper is oxidized to CuCl by exceeding the solubility equilibrium between CuCl and $CuCl_2$ (ref. 26). So there is a gradual increase of potential, because the insoluble CuCl is deposited on the copper surface. This results in passivation of copper surface. The dissolved oxygen in the electrolytic solution is reduced on copper surface. It is a good approximation to the evolution of hydrogen and only considers the reduction of oxygen in both HCl and NaCl electrolytic solutions at potentials near the corrosion potential.

The deposition of MOSTY SAM on the copper surface shifted the corrosion potential of copper cathodically and also reduces the corrosion current
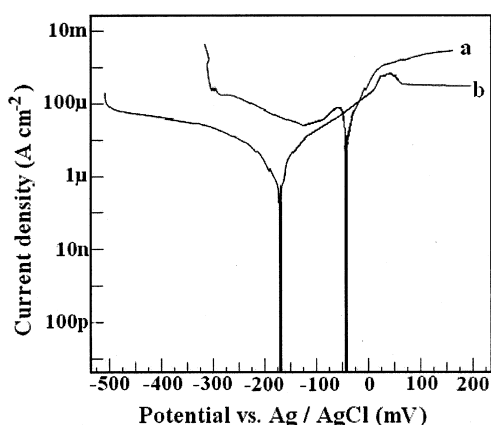


Fig. 2 — Potentiodynamic polarization curves in 0.02 M aq. HCl (a) Bare copper, (b) SAM covered copper
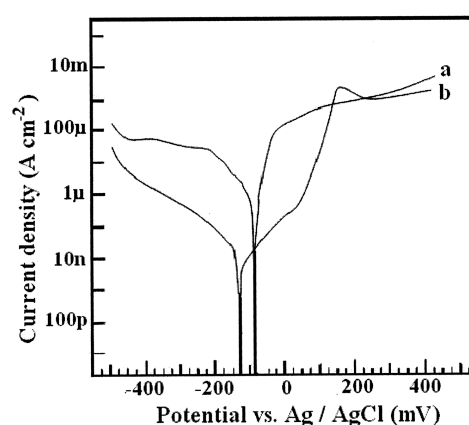


Fig. 3 — Potentiodynamic polarization curves in 0.02 M aq. NaCl. (a) Bare copper, (b) SAM covered copper

densities, which are shown in Figs 2 and 3. The cathodic reaction is inhibited to a larger extent than the anodic reaction. Since the transfer of oxygen from the bulk solution to the copper interface will strongly affect the rate of oxygen reduction, it can be inferred that the SAM is behaving as cathodic inhibitor to copper corrosion by arresting the transfer of $O_2$ to the cathodic sites of the Cu surface and also by arresting Cu dissolution by Cl⁻ ions[28]. The mercapto group in the MOSTY binds to the copper surface via thiolate bond, while the long hydrophobic alkyl chain constitutes the ultrathin protective film, which is densely packed. This film completely insulates the underlying copper surface[29]. The corrosion inhibition efficiencies (IE) of MOSTY SAM on copper from the polarization studies have been calculated by using Eq. (4)[30].

$$IE\ (\%) = (i_{corr} - i^1_{corr}) \times 100/i_{corr} \qquad \ldots(4)$$

where $i_{corr}$ and $i^1_{corr}$ are the corrosion current densities of the bare copper specimen and the SAM coated copper specimen respectively. The inhibition efficiencies obtained from these results are in good agreement with those from weight-loss studies and infer that the MOSTY SAM offers good protection to copper from corrosion. These results are also in good agreement with the previous results available in the literature for different SAMs on copper surface[11,28,31,32].

**Electrochemical impedance studies**

Impedance studies are used to characterize the properties of SAM[11,12,30-33]. The method is based on the measurement of the response of the electrochemical cell to an alternating potential of small amplitude[34]. Nyquist plots of SAM covered copper electrodes have been obtained in 0.02 M HCl and 0.02 M NaCl aqueous solutions after 30 min equilibration, since the open-circuit potentials of the electrodes became steady within 30 min. The impedance spectra were reported in the literature by measuring at the corresponding open-circuit potentials[35]. The Nyquist plots for the bare copper and the SAM covered copper in 0.02 M aq. HCl solutions are shown in the Fig. 4. The Nyquist plots of bare copper specimen in 0.02 M aq. HCl exhibit warburg impedance indicating the mass transfer, which greatly affects the corrosion reactions. In the case of SAM covered copper specimen, the corrosion reactions do not take place. Therefore, the warburg impedance of the SAM coated copper specimen disappeared in the

lower frequency region[11,35]. The high frequency capacitative loop can be attributed to the time constant of the charge transfer resistance ($R_t$) and the double layer capacitance ($C_{dl}$)[29,36].

Figure 5 shows the impedance spectra of the bare copper and the SAM covered copper in 0.02 M aq. NaCl solution. Like in HCl, the impedance of MOSTY SAM covered copper specimen in 0.02 M NaCl is also higher than the bare copper, which is suggestive of no corrosion reactions. Because of this phenomenon the warburg impedance of MOSTY SAM coated copper specimen disappeared at lower frequency region. Zamborini and Crooks[37] proposed a corrosion reaction model for the electrode covered by SAMs with defects. In this model, the corrosive ions, such as halide ions, can permeate through the defects of the SAMs and react with the metal substrate, giving rise to the expansion of the defective sites and leading to further destruction of SAMs. Long hydrocarbon chains within the SAM can partially heal the defects. MOSTY contains long hydrocarbon chain (octadecyl), one sulphur atom and four nitrogen atoms, which all together form a protective monolayer on the copper surface. This protective monolayer
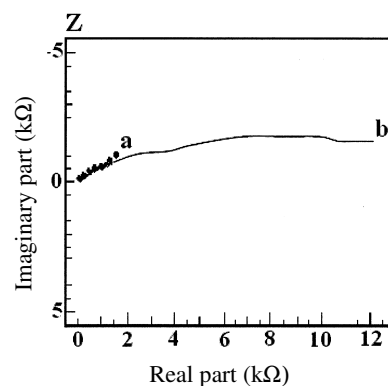
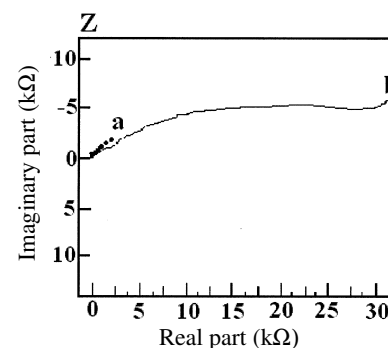Fig. 4 — Nyquist plots in 0.02 M aq. HCl. (a).bare copper, (b) SAM covered copper

Fig. 5 — Nyquist plots in 0.02 M aq. NaCl. (a).bare copper, (b) SAM covered copper

prevents the permeation of corrosive ions to the surface of copper and thereby protects it from corrosion. To analyze the impedance plots for the bare and MOSTY SAM covered copper specimen two equivalent circuits are proposed, which are shown in Figs 6a and 6b respectively.

To obtain a good fit of the Impedance data, the capacitance is substituted by constant phase element (CPE). The impedance of a CPE is given by Eq. (5).

$$Z_{CPE} = 1/ Y_0 (j\omega)^{-n} \qquad \ldots(5)$$

Here, $\omega$ is angular frequency; $Y_0$ is magnitude of CPE and n is the exponential[38]. The impedance parameters obtained from Nyquist plots are shown in Table 2. The inhibition efficiency of MOSTY SAM has been calculated by using the charge transfer resistance ($R_t$) with the help of Eq. (6).

$$IE\ (\%) = (R_t - R^1_t) \times 100 / R_t \qquad \ldots(6)$$

where $R_t$ = charge transfer resistance of SAM covered copper substrate, $R^1_t$ = resistance of the bare copper substrate. The results revealed that the MOSTY SAM formed on the copper surface is a good inhibitor for cop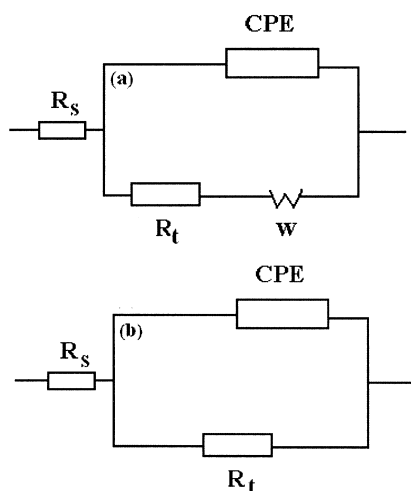per corrosion. The inhibition efficiencies obtained by weight-loss studies, potentiodynamic polarization studies and impedance studies are in good agreement with each other.

**X-ray photoelectron spectral analysis**

The XPS of the SAM formed on the copper surface by using MOSTY may be interpreted as follows. The computer deconvolution spectra for nitrogen, sulphur and carbon present in the SAM are shown in the Figs 7a, b and c respectively. Figure 7a shows 2 peaks appeared due to N 1s electron at 399.1 and 400.3 eV respectively while the characteristic binding energy of the elemental nitrogen is reported as 398.0 eV in the literature[38,39]. These two peaks correspond to two different kinds of nitrogen environment present in the MOSTY SAM. The peaks at 399.1 and 400.3 eV are attributed to the neutral imine (–N=) and amine (–N–H) nitrogen atoms[40,41]. The shifts indicate the chemisorption and complex formation of MOSTY SAM through nitrogen with Cu$^+$ ion available on the anodic site. Similar shifts are reported in the studies using substituted thio pyrimidines as inhibitors for copper[42].

The X-ray photoelectron spectrum of S 2p electron is shown in Fig. 7b. The peak at 162.6 eV is due to the S 2p$_{3/2}$ electron and the one at 163.8 eV is due to the S 2p$_{1/2}$ electron, while the characteristic elemental binding energy reported in the literature for the S 2p electron is 164.0 eV[43]. Thus there is a shift of binding energy of 2p electron of S, which is present in the surface film on the copper surface. It has been reported in the literature by several workers in this field[44-46] that the S 2p peak centered around 162.5 eV is typical of the thiolate bonds, Cu-S- and in such a case the intensity ratio between the components of S 2p$_{3/2}$ and S 2p$_{1/2}$ must be nearly equal to 2.2. It may be noted that in the XPS spectrum of S 2p in the presence of MOSTY, the intensity ratio between the S 2p$_{3/2}$ and S 2p$_{1/2}$ components is found to be 2.4. Thus it can be inferred that there is chemisorption of MOSTY on copper surface through the thiolate bond and the subsequent formation of a complex between the MOSTY and Cu$^+$ ion to form a protective film.



Fig. 6 — Equivalent circuits used in impedance measurements, (a) for bare copper, (b) for SAM covered copper

Table 2 — Corrosion parameters from potentiodynamic polarization and impedance studies

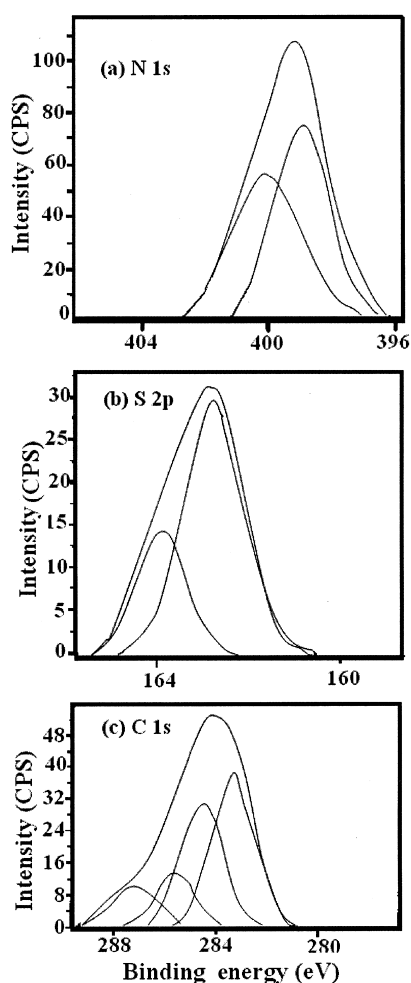| S. No | Specimen | Corrosive environment | $E_{corr}$ (mV) vs. Ag/AgCl | $i_{corr}$ ($\mu$A/ cm$^2$) | IE (%) (cm$^2$) $i_{corr}$ | $b_a$ (mV/decade) | $b_c$ (mV/decade) | $R_t$ (k$\Omega$) | IE (%) (from $R_t$) |
|---|---|---|---|---|---|---|---|---|---|
| 1 | Bare copper | 0.02 M HCl | -42.77 | 13.10 | -- | 46.6 | -591 | 2.03 | -- |
| 2 | SAM covered copper | 0.02 M HCl | 165.40 | 1.64 | 87.48 | 88.3 | -115 | 13.17 | 84.58 |
| 3 | Bare copper | 0.02 M NaCl | -83.45 | 11.90 | -- | 80.8 | - 433 | 3.21 | -- |
| 4 | SAM covered copper | 0.02 M NaCl | -132.90 | 0.21 | 98.27 | 128.0 | -133 | 33.75 | 90.49 |

Fig. 7 — X-ray photoelectron spectra of the elements present in the SAM. (a) N 1s, (b) S 2p, (c) C 1s

The peaks of C 1s electron present in the SAM are shown in Fig. 7c. The peak at 285.72 eV is due to the −C−N bond and the peak at 287.26 eV is due to the −C−S bond[40]. Thus there is a shift in the binding energy value from 284.0 eV (ref. 47), which is the value of C 1s in elemental form. The binding energy values of 283.30 and 284.57 eV are due to carbon atom in aliphatic chain[48]. Thus the MOSTY SAM formed on copper surface is characterized by XPS, which clearly infers the chemisorption of MOSTY on copper and subsequent complex formation to form a protective film.

## Conclusion

The studies concluded that the SAM formed by 3-methyl-5-octadecylsulfanyl-[1,2,4]triazole-4-yalamine on copper surface offers excellent protection from corrosion in 0.02 M aq. HCl and 0.02 M aq. NaCl solutions. The inhibition efficiencies obtained from weight-loss studies, potentiodynamic polarization studies and electrochemical impedance studies are in good agreement with each other. The mechanistic aspects of the corrosion inhibition are explained by the results of electrochemical and surface analytical studies. The self assembled monolayer of 3-methyl-5-octadecylsulfanyl-[1,2,4]triazole-4-ylamine on copper surface acts as a protective film and protects the metal from corrosion in the chosen aggressive environments.

## Nomenclature

$C_{dl}$   =  Double layer capacitance
CPE   =  Constant phase element
$E_{oc}$   =  Open circuit potential
IE   =  Inhibition efficiency
$i_{corr}$   =  Corrosion current density of bare copper
$i^1_{corr}$   =  Corrosion current density of SAM covered copper
$R_t$   =  Charge transfer resistance of SAM covered copper
$R^1_t$   =  Charge transfer resistance of bare copper
$\Delta W$   =  Weight-loss of the bare copper
$\Delta W_1$   =  weight-loss of the SAM covered copper
ω   =  Angular velocity
$Y_0$   =  Magnitude of CPE
Z   =  Impedance

## References

1   Kane Jennings G & Paul E Laibins, *Colloids and Surfaces A: Physicochem & Eng Asp*, 116 (1996) 105.
2   Ma H Y, Yang C, Yin B S, Li G Y, Chen S H & Luo J L, *Appl Surface Sci*, 218 (2003) 143.
3   Sayed EI & Sherif M, *Appl Surface Sci*, 252 (2006) 8615.
4   Yan C W, Lin H C & Cao C N, *Electrochim Acta*, 45 (2000) 2815.
5   Flink S, Boukamp B A, Van den Berg A, Van Veggel F C J M & Reinhoudt D N, *J Am Chem Soc*, 120 (1998) 4652.
6   Everett W R & Fritsch-Faules I, *Anal Chim Acta*, 307 (1995) 253.
7   Yang W, Gooding J J & Hibbert D B, *J Electroanal Chem*, 516 (2001) 10.
8   Vastag Gy, Szocs E, Shaban A & Kalman E, *Pure Appl Chem*, 73 (2001) 1861.
9   Feng Y, Teo W K, Siow K S, Gao Z, Tan K L & Hsieh A K, *J Electrochem Soc*, 144 (1997) 55.
10  Itoh M, Nishahara H & Aramaki K, *J Electrochem Soc*, 142 (1995) 1839.
11  Yamamoto Y, Nishahara H & Aramaki K, *J Electrochem Soc*, 140 (1993) 436.
12  Laibinis P E & Whitesides G M, *J Am Chem Soc*, 114 (1992) 105.
13  Quan Z, Wu X, Chen S, Zhao S & Ma H, *Corrosion*, 57 (2001) 195.
14  Quan Z, Chen S, Cui X & Li Y, *Corrosion*, 58 (2002) 248.
15  Tremont R J, De Jesu´s-Cardona H, Garcı´a-Orozco J, Castro R J & Cabrera C R, *J Appl Electrochem*, 30 (2000) 737.
16  Da-Quan Zhang, Li-Xin Gao & Guo-ding Zhou, *Corros Sci*, 46 (2004) 3031.
17  Yong Sheng Zhao, Wensheng Yang, Guangjin Zhang, Ying Ma & Jiannian Yao, *Colloids and Surfaces A: Physicochem & Eng Asp*, 277 (2006) 111.

18  Audrueth L F, Scott E S & Kippur P S, *J Org Chem*, 19 (1954) 733.
19  Baeyer H & Kroger E F, *Ann*, 637 (1969) 135.
20  Reid J R & Heindel N D, *J Heterocycl Chem*, 13 (1976) 925.
21  Cicileo G P, Rosales B M, Varela F E & Vilche J R, *Corros Sci*, 41 (1999) 1359.
22  Freeman R A & Silverman D C, *Corrosion*, 48 (1992) 463.
23  Lee H P & Nobe K, *J Electrochem Soc*, 120 (1998) 13452.
24  Braun M & Nobe K, *J Electrochem Soc*, 126 (1979) 1666.
25  Bemedetti A V, Sumodjo P T A, Nobe K, Cabot P L & Proud W G, *Electrochim Acta*, 40 (1995) 2657.
26  Tromans D & Sun R H, *J Electrochem Soc*, 138 (1991) 3235.
27  Baracella L & Griess J C (Jr), *J Electrochem Soc*, 120 (1973) 459.
28  Itoh M, NIshahara H & Aramaki K, *J Electrochem Soc*, 142 (1995) 1839.
29  Feng Y, Teo W K, Siow K, Gao Z, Tao K L & Hsieh A K, *J Electrochem Soc*, 144 (1997) 55.
30  Ma H, Chen S, Niu L, Shang S, S.Zhao, Li S & Quan Z, *J Electrochem Soc*, 148 (2001) 13208.
31  Ishibashi M, Itoh M, Nishahara H & Aramaki K, *Electrochim Acta*, 41 (1996) 241.
32  Haneda R, Nishahara H & Aramaki K, *J Electrochem Soc*, 144 (1997) 1215.
33  Chun-Tao Wang, Shen-Hao Chen, Hou-Yi Mai Lan Hua & Nai-Xing Wang, *J Serb Chem Soc*, 67 (2002) 685.
34  Tan Y S, Srinivasan M P, Pehkonen S O & Simon Y M Chooi, *Corros Sci*, 48 (2006) 840.
35  Wang C T, Chen S H, Ma H Y & Qi C S, *J Appl Electrochem*, 33 (2003) 179.
36  Feng Y, Teo W K, Siong K S, Tan K L & Hsieh A K, *Corros Sci*, 38 (1996) 369.
37  Zamborini F P & Crooks R M, *Langmuir,* 14 (1998) 3279.
38  Beccaria A M & Bertolotto C, *Electrochim Acta*, 42 (1997) 1361.
39  *XPS Hand Book* (V.G. Scientific Ltd., West Sussex, England), 1989.
40  Sinapi F, Delhalle J & Mekhalif Z, *Mater Sci Eng*, 22 (2002) 345.
41  Azhar M EL, Traisnel M, Mernary B, Gengembre L, Bentiss F & Lagrenee M, *Appl Surf Sci*, 185 (2002) 197.
42  Meneguzzi A, Ferreira C A, Pham M C, Delamar M & La-caze P C, *Electrochim Acta*, 44 (1999) 2149.
43  Mudler J F, Stickle W F, Sobol P E & Boben K D, *Hand Book of X-ray Photoelectron Spectroscopy* (Physical Electronics Inc, Minesota), 1995.
44  Myung M Sung & Yunsoo Kim, *Bull Korean Chem Soc*, 22 (2001) 7.
45  Sinapi F, Lejeune I, Delhalle J & Mekhalif Z, *Electrochim Acta*, 52 (2007) 5182.
46  Mekhalif Z, Sinapi F, Laffineur F & Delhalle J, *J Electron Spectrosc Relat Phenom*, 121 (2001) 149.
47  Taneichi D, Haneda R & Aramaki K, *Corros Sci*, 43 (2001) 1589.
48  Sastry V S, *Corrosion Inhibitors-Principles and Applications* (John Wiley & Sons, New York), 1998.